Electronic Supplementary Information (ESI)

Positional Isomeric Effect of Monobrominated Ending Groups within Small Molecule Acceptors on Photovoltaic Performance

Wei Wang, [a†] Gongchun Li, [a†] Yuhao Li, [b] Chun Zhan, [a] Xinhui Lu [*b] and Shengqiang Xiao [*a]

[a] State Key Laboratory of Advanced Technology for Materials Synthesis and Processing, Wuhan University of Technology, Wuhan 430070, P. R. China.

[b] Department of Physics, The Chinese University of Hong Kong, Sha Tin, Hong Kong SAR 999077, China.

*Corresponding author, E-mail: shengqiang@whut.edu.cn (S.X.), xinhui.lu@cuhk.edu.hk (X.L.)

[†] Wei Wang and Gongchun Li contributed equally to this work.

Contents

(under AM 1.5G illumination) processed from the CB solution with 0.5% CN (v/v) and later thermally annealed at different temperature (**Table S6**).

(l) Photovoltaic parameters of the PBDB-T-2Cl:BDSeTICBr-m (1:1, w/w) devices (under AM 1.5G illumination) processed from the CB solution with 0.5% CN (v/v) and later thermally annealed at different temperature (**Table S7**).

(m) The optimized photovoltaic parameters of the PBDB-T-2Cl: SMA (1:1, w/w) devices processing with the additive CN (v/v, in CB), TA and CN+TA under AM 1.5G illumination **(Table S8)**.

(n) The typical *J-V* curves of the optimized PSCs under AM 1.5G irradiation (**Fig. S19**).

(o) Photogenerated current density versus effective voltage curves under AM 1.5G illumination (a) and J-V curves from -3 V to +3 V in dark (b) (Fig. S20).

(p) $J_{0.5}$ vs V ($V = V_{\mathrm{appl}}-V_{\mathrm{bi}}-V_{\mathrm{rs}}$) plots for electron-only (a) and hole-only (b) devices of the PBDB-T-2Cl:SMA blends (**Fig. S21**).

(q) GISAXS patterns of the PBDB-T-2Cl:BDSeTICBr-γ (a), PBDB-T-2Cl:BDSeTICBr-δ (b) and PBDB-T-2Cl:BDSeTICBr-m (c) film (**Fig. S22**).

(r) GISAXS in-plane profiles of the PBDB-T-2Cl:SMA blend films and their model fittings with the Debye-Anderson-Brumberger (DAB) model (**Fig. S23**).

(s) The calculated domain sizes from GISAXS within the PBDB-T-2Cl:BDSeTICBr-γ, PBDB-T-2Cl:BDSeTICBr-δ and PBDB-T-2Cl:BDSeTICBr-m film (**Table S9**).

(t) AFM height images (a), (b), (c) and phase images (d), (e), (f) for the PBDB-T-2Cl:BDSeTICBr-γ, PBDB-T-2Cl:BDSeTICBr-δ and PBDB-T-2Cl:BDSeTICBr-m film, respectively (**Fig. S24**).

(u) GIWAXS scattering patterns of the neat films of PBDB-T-2Cl, BDSeTICBr-γ, BDSeTICBr-δ and BDSeTICBr-m and their PBDB-T-2Cl:SMA blend films (**Fig. S25**).

(v) GIWAXS characteristics of the neat films of PBDB-T-2Cl, BDSeTICBr-γ, BDSeTICBr-δ and BDSeTICBr-m and their PBDB-T-2Cl:SMA blend films. (**Table S10**).

1. Materials.

IC-Br-m[1], BDSeT-2CHO[2], and polymer PBDB-T-2Cl[3] were synthesized according to previously reported approaches. The ZnO precursor was prepared according to the published literature.[4] All other reagents were purchased from *J&K*, *Alfa Aesar,* and *Energy*. All solvents for reactions were freshly distilled immediately prior to use.

2. Measurements and Instruments.

^{1}H and ^{13}C NMR spectra were performed on a Bruker AV500 at 500 MHz using deuterated chloroform ($CDCl_3$) as the solvent. Mass spectroscopy (MS) was recorded by using a Waters SYNAPT G2-Si HDMS for MALDI-TOF. UV−vis spectra were measured on a SHIMADZU UV-1750 spectrophotometer. Cyclic voltammetry (CV) experiments were performed with a CHI 660D analyzer. All CV measurements were carried out in 0.1 M tetrabutylammonium hexafluorophosphate (Bu_4NPF_6) in anhydrous acetonitrile with a conventional three-electrode configuration employing a platinum wire as the counter electrode, platinum electrode coated with a thin polymer film as the working electrode, and Ag/Ag^+ electrode as the reference electrode at a scan rate of 80 mV s^{-1}. The film thickness was measured by a Dektak XT profilometer from Bruker. The photoluminescence (PL) spectrum of films spin-coated on precleaned quartz glass was performed on a Fluoro Max-3-P spectrometer. The atomic force microscopy (AFM) images (5.0 μm × 5.0 μm) were obtained through tapping mode on Multimode 8 SPM at ambient conditions. RTESPA (0.01-0.025 ohm-cm Antimony (n) doped silicon) tips with a spring constant of 20-80 N m^{-1} and a frequency of 305-356 kHz was used in imaging. The grazing incident wide-angle X-ray scattering (GIWAXS) and grazing incidence small-angel X-ray scattering (GISAXS) measurement was carried out with a Xeuss 2.0 SAXS/WAXS laboratory beamline using a Cu X-ray source (8.05 keV, 1.54 Å) and a Pilatus3R 300K detector.

3. Fabrication and Characterization of Polymer Solar Cells.

The PSC devices were fabricated in the inverted configuration of ITO (150 nm)/ZnO (~35nm)/ PBDB-T-2Cl: SMA/MoO_3 (~8 nm)/Ag (~100 nm). Firstly, glass substrates with patterned ITO (~150 nm thickness) were cleaned by ultrasonic treatment sequentially in distilled water, acetone, and isopropanol for 20 min before UV-Ozone cleaning (10 min). The ZnO precursor was spin-coated onto the ITO substrates at 4000 rpm for 40 s and baked at 150 °C for 1 hour in the air to obtain a thin layer of ZnO (~ 35nm). The polymer PBDB-T-2Cl was dissolved in chlorobenzene (CB) with a fixed concentration of 10 mg mL^{-1} and then followed by blending with SMAs in various weight ratios in a glove box. The blend solutions were stirred at 70 ^{o}C for 8 hours and cooled to room temperature. The spin-coating of all the BHJ blend films was conducted in the glovebox filled with N_2. For the blended solutions with a specific D:A weight ratio, the spinning speeds were chosen from 400 to 1000 rpm to obtain films with different thicknesses. The spin-coating processes were started right on the chosen speeds and stopped after 60 s with natural acceleration and deceleration respectively. The as-prepared films were then left in the glovebox and dried naturally over 1 hour at room temperature. MoO_3 (8 nm) and Ag (100 nm) were then sequentially deposited on the top of these BHJ films as the anode at a pressure of 2×10^{-6} mbar through a shadow mask that defines 8 devices with each active area of 0.09 cm^2. In this as-cast condition, the PBDB-T-2Cl: SMA blends all obtained their best performance at the D:A weight ratio of 1:1 with the spinning speed at 600 rpm. Thus, these D:A weight ratio (1:1) and the spinning speed (600 rpm) were applied for further optimization on film-processing. Under the thermal annealing (TA) condition, the as-prepared blend films right after stopping spin-coating were directly placed on a hot plate to be thermally annealed at various temperatures ranging from 100 to 180 °C for 10min. Under 1-chloronaphthalene (CN) additive condition, CN with different volume ratios to CB was added to the blend solutions with optimized D:A weight ratio of PBDB-T-2Cl:SMA. The spin-coating parameters were conducted in the same way as used for the original BHJ blend films without the additive. Right after the spin-coating, the as-prepared blend films were solidified naturally over 1 hour at room temperature. Under the processing condition of combining the addition of additive and TA, the as-prepared BHJ blend films from the solution with CN were directly placed on a hot plate to be thermally annealed at various temperatures ranging from 100 to 180 °C for 10 min instead of drying naturally.

Current-voltage measurements were carried out in a glovebox under AM 1.5 G irradiation (100 mW cm^{-2}) from a 450 W solar simulator (Newport 94023A-U) calibrated by a NREL certified standard silicon cell. Current versus potential (*J*-*V*) curves were recorded with a Keithley 2420 digital source meter. The EQE measurement was performed on a QEX10 (PV Measurements, Inc.) system equipped with a standard Si solar cell (Oriel, VLSI standards) across a wavelength range of 300-900 nm.

The SCLC *J-V* curves were obtained in the dark from the electron-only devices of ITO/ZnO (~35nm)/BHJ/Ca (~30nm)/Al (~80nm) and the hole-only devices of ITO/PEDOT:PSS (~40nm)/BHJ/MoO_3 (~8nm)/Ag (~100nm). The electron and hole mobilities were calculated using the Mott-Gurney square law: $J = (9/8)\varepsilon_0\varepsilon_r\mu(V^2/L^3)$ where ε_0 is vacuum permittivity, ε_r is the dielectric constant of the polymer used, μ is the charge ESI-5 carrier mobility, V is the effective applied voltage, and L is the thickness of the active film in the device. The fabrication of electron-only devices: a thin layer (~35 nm) of ZnO was prepared as introduced above. The blend films were then spin-coated from the blend solution in the glovebox filled N_2 and processed according to the optimized film processing parameters under TA or CN+TA conditions. Ca (~30 nm) and Al (~80 nm) were then sequentially evaporated and deposited on the top of blend films as the cathode at a pressure of 2×10^{-6} mbar. The fabrication of hole-only devices: a thin layer (~40 nm) of PEDOT:PSS (PH1000) was spin-coated onto the ITO substrates at 4000 rpm for 60 s and baked at 150 °C for 30 min in air. Subsequently, the blend films were spin-coated from the blend solution in the glovebox filled N_2 and processed according to the optimized film processing parameters under TA or CN+TA conditions. MoO_3 (~8 nm) and Ag (~100 nm) were then sequentially evaporated and deposited on the top of blend films as the cathode at a pressure of 2×10^{-6} mbar.

4. Synthesis of Compounds.

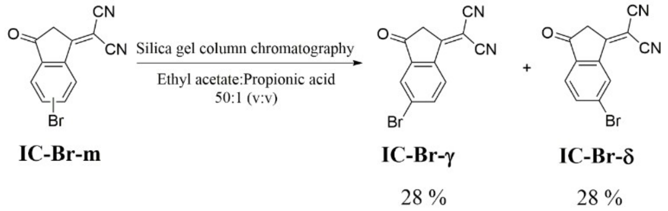

IC-Br-γ and IC-Br-δ. IC-Br-m (2 g) was purified by column chromatography on silica gel (ethyl acetate/ propionic acid, v/v, 50/1). It needs to be noted that IC-Br-m was separated in batches with a small amount. IC-Br-γ was eluted out before IC-Br-δ (Fig. S34). The collected solution with either of the products was then neutralized with 5% $NaHCO_3$ solution, washed with brine and water, and dried over anhydrous $MgSO_4$. Removal of the solvent under reduced pressure offered the pure solid product. The pure IC-Br-γ (599 mg) and IC-Br-δ (602 mg) were obtained both with a yield of ~ 30%. IC-Br-γ ^{1}H NMR (500 MHz, $CDCl_3$), δ (ppm): 8.50 (d, J = 8.50 Hz, 1H), 8.10 (d, J = 1.80 Hz, 1H), 7.99 (m, 1H), 3.74 (s, 2H). ^{13}C NMR (125 MHz, $CDCl_3$), δ (ppm): 193.34, 164.92, 141.65, 140.89, 139.12, 131.54, 127.94, 127.03, 112.01, 111.84, 79.60, 43.20. IC-Br-δ ^{1}H NMR (500 MHz, $CDCl_3$), δ (ppm): 8.77 (s, 1H), 7.96 (d, J = 8.15 Hz, 1H), 7.83 (d, J = 8.20 Hz, 1H), 3.73 (s, 2H). ^{13}C NMR (125 MHz, $CDCl_3$), δ (ppm): 193.51, 164.56, 143.61, 139.01, 138.89, 131.76, 128.86, 125.70, 111.62, 80.42, 43.16.

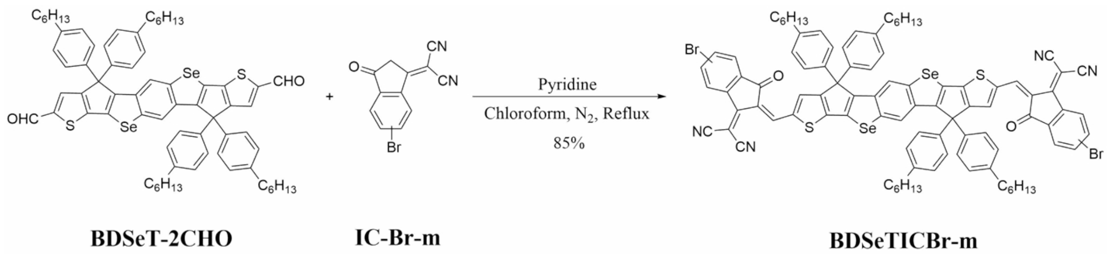

BDSeTICBr-m. BDSeT-2CHO (234mg, 0.2 mmol) and IC-Br-m (164 mg, 0.6 mmol) were dissolved in 40 mL of dry chloroform under nitrogen atmosphere. Then, pyridine (2 mL) was added in and the reactants were heated to reflux for 12 hours with stirring. After removal of the solvent under reduced pressure, the reaction mixture was directedly purified by silica gel chromatography with chloroform as the eluent. The pure product was a dark blue solid (285 mg, yield 85%).^{1}H NMR (500 MHz, $CDCl_3$), δ (ppm): 8.85 (d, J = 3.15 Hz, 2H), 8.80 (s, 1.1H), 8.51 (d, J = 8.40 Hz, 0.9H), 8.02 (s, 2H), 7.96 (s, 0.9H), 7.82 (t, J = 8.70 Hz, 2H), 7.73 (d, J = 8.00 Hz, 1.1H), 7.67 (s, 2H), 7.15 (d, J = 8.00 Hz, 8H), 7.10 (d, J = 8.00 Hz, 8H), 2.56 (t, J = 7.60 Hz, 8H), 1.59-1.55 (m, 12H), 1.34-1.28 (m, 24H), 0.87-0.85 (m, 12H). ^{13}C NMR (125 MHz, $CDCl_3$), δ (ppm): 187.38, 186.98, 162.76, 159.36, 159.16, 158.72, 144.58, 142.65, 141.23, 140.65, 138.52, 138.20, 137.29, 136.73, 135.34, 133.36, 130.18, 129.56, 128.86, 128.58, 128.12, 126.42, 124.62, 123.11, 120.86, 114.46, 114.32, 69.20, 68.65, 63.75, 35.53, 31.65, 31.20, 29.08, 22.56, 14.07. MALDI-TOF (MS) for $C_{94}H_{80}Br_2N_4O_2S_2Se_2$: Calcd 1678.24; found 1680.26 ($M+2H^+$).

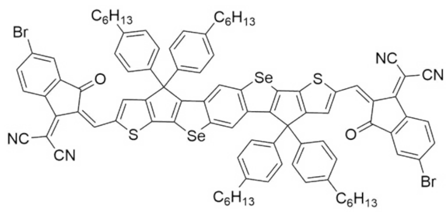

BDSeTICBr-γ

BDSeTICBr-γ. The compound was synthesized according to the same procedure for BDSeTICBr-m by the reaction of BDSeT-2CHO (234mg, 0.2 mmol) and IC-Br-γ (164 mg, 0.6 mmol) . The pure product was obtained as a dark blue solid (296 mg, yield 88%).^{1}H NMR (500 MHz, $CDCl_3$), δ (ppm): 8.86 (s, 2H), 8.52 (d, J = 8.40 Hz, 2H), 8.02 (s, 2H), 8.02 (s, 2H), 7.99 (s, 2H), 7.84 (d, J = 8.30 Hz, 2H), 7.67 (s, 2H), 7.15 (d, J = 8.15 Hz, 8H), 7.10 (d, J = 8.25 Hz, 8H), 2.56 (t, J = 7.65 Hz, 8H), 1.65-1.59 (m, 12H), 1.30-1.27 (m, 24H), 0.89-0.84 (m, 12H). ^{13}C NMR (125 MHz, $CDCl_3$), δ (ppm): 187.03, 159.38, 142.67, 140.63, 138.42, 138.25, 136.75, 133.37, 129.57, 128.88, 128.13, 126.45, 120.83, 113.46, 89.64, 68.67, 63.76, 35.54, 31.67, 31.21, 29.32, 29.10, 22.57, 14.07. MALDI-TOF (MS) for $C_{94}H_{80}Br_2N_4O_2S_2Se_2$: Calcd 1678.24; found 1680.26 (M+2H$^+$).

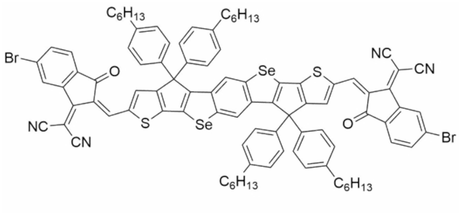

BDSeTICBr-δ

BDSeTICBr-δ. The compound was synthesized according to the same procedure for BDSeTICBr-m by the reaction of BDSeT-2CHO (234mg, 0.2 mmol) and IC-Br-δ (164 mg, 0.6 mmol). The pure product was a dark blue solid (292 mg, yield 87%).^{1}H NMR (500 MHz, $CDCl_3$), δ (ppm): 8.85 (s, 2H), 8.80 (d, J = 1.35 Hz, 2H), 8.02 (s, 2H), 7.83 (m, 2H), 7.74 (d, J = 8.00 Hz, 2H), 7.67 (s, 2H), 7.15 (d, J = 8.40 Hz, 8H), 7.10 (d, J = 8.40 Hz, 8H), 2.57-2.54 (m, 8H), 1.59-1.56 (m, 12H), 1.34-1.26 (m, 24H), 0.87-0.85 (m, 12H). ^{13}C NMR (125 MHz, $CDCl_3$), δ (ppm): 187.37, 162.76, 159.37, 159.17, 158.70, 144.58, 142.64, 141.22, 140.65, 138.57, 138.52, 138.20, 137.28, 136.73, 135.33, 133.35, 130.18, 129.67, 128.86, 128.20, 128.11, 124.61, 123.11, 120.85, 114.46, 114.32, 69.19, 63.74, 35.52, 31.65, 31.20, 29.08, 22.55, 14.07. MALDI-TOF (MS) for $C_{94}H_{80}Br_2N_4O_2S_2Se_2$: Calcd 1678.24; found 1680.26 (M+2H$^+$).

5. Supplementary figures and tables

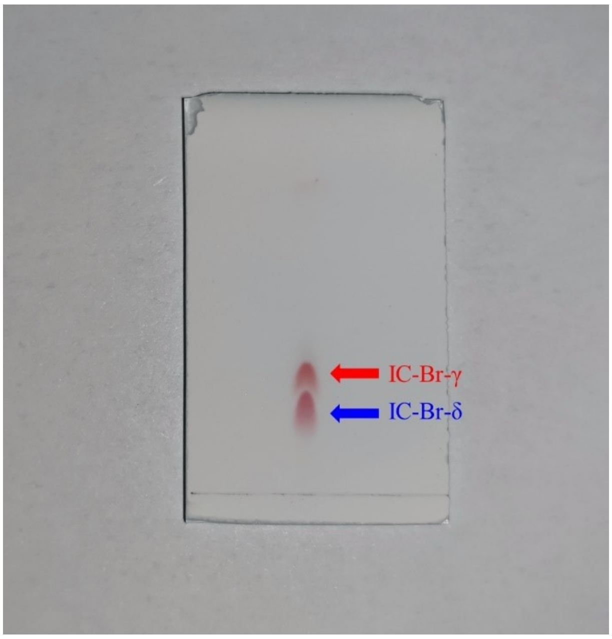

Fig.S1 The thin layer chromatography (TLC) picture of IC-Br-m with ethyl acetate: propionic acid (v:v = 50:1) as the eluent.

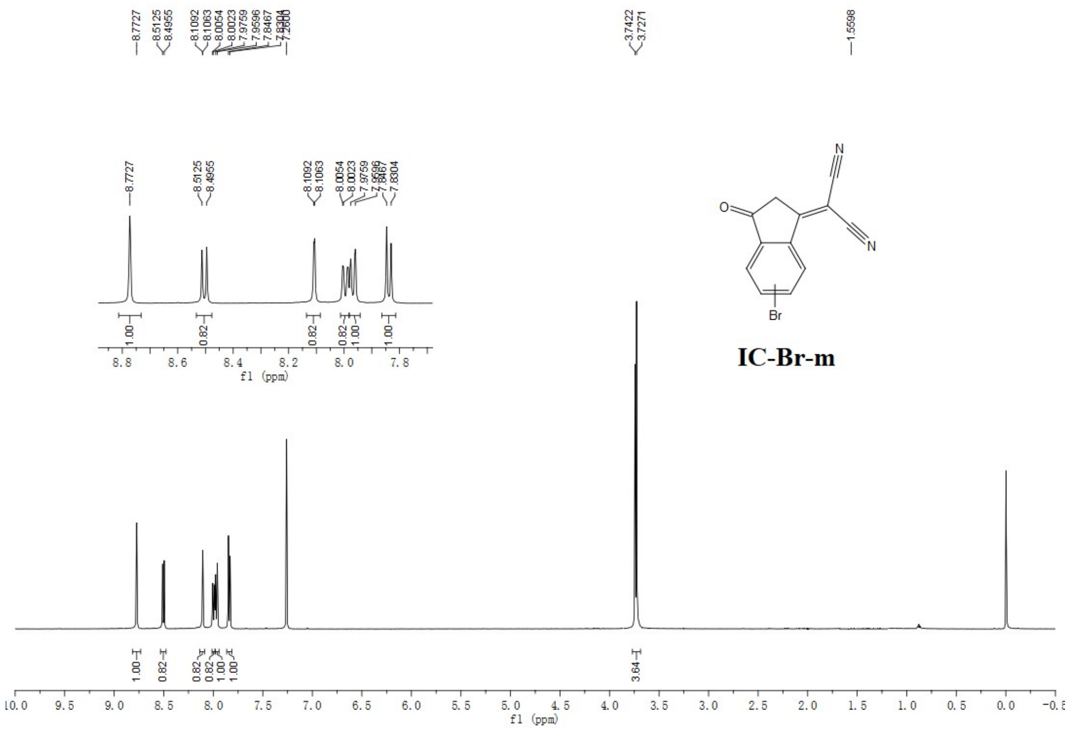

Fig.S2 The ^{1}H NMR spectrum of IC-Br-m.

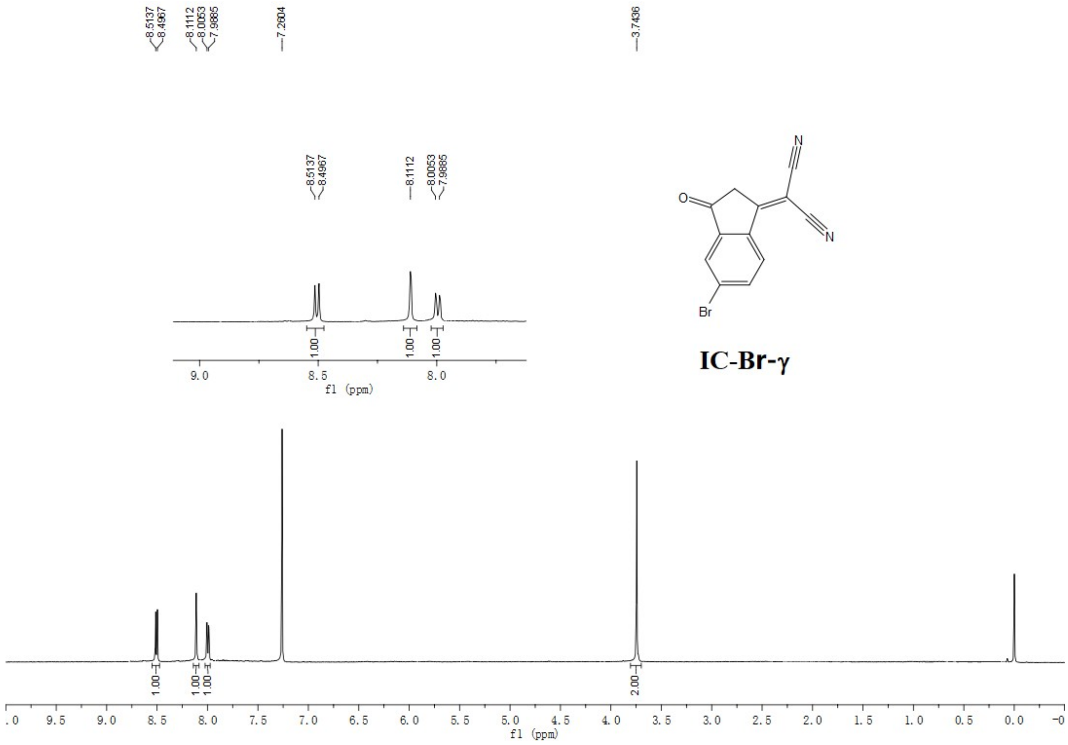

Fig.S3 The ^{1}H NMR spectrum of IC-Br-γ.

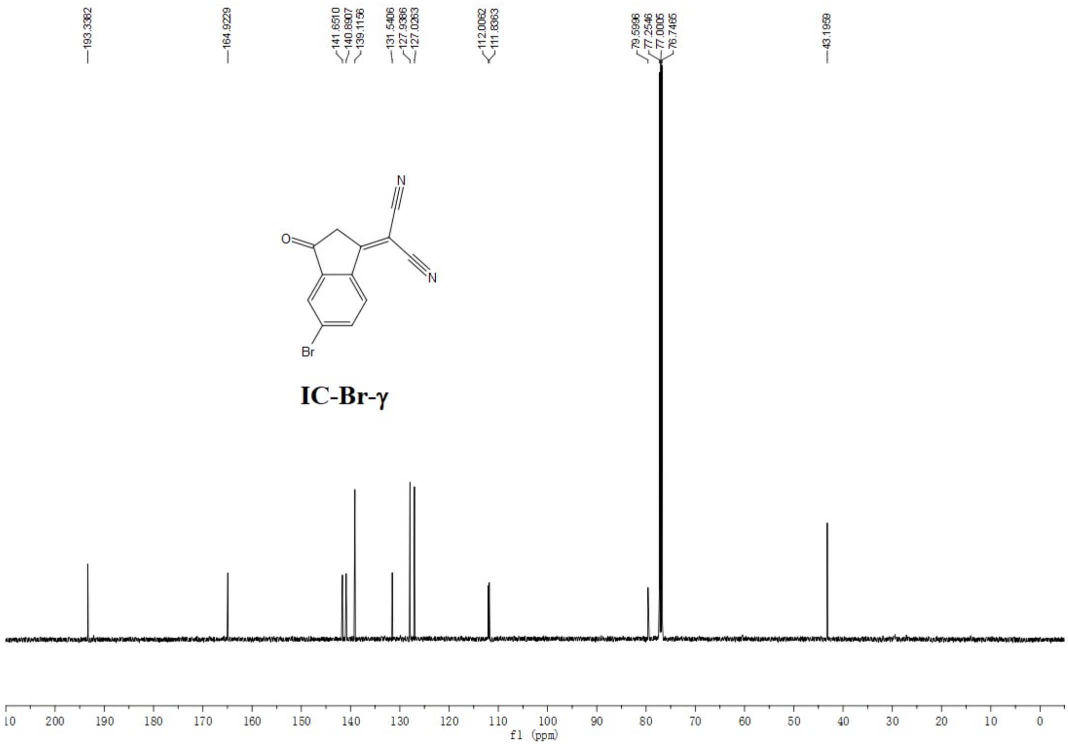

Fig.S4 The ^{13}C NMR spectrum of IC-Br-γ.

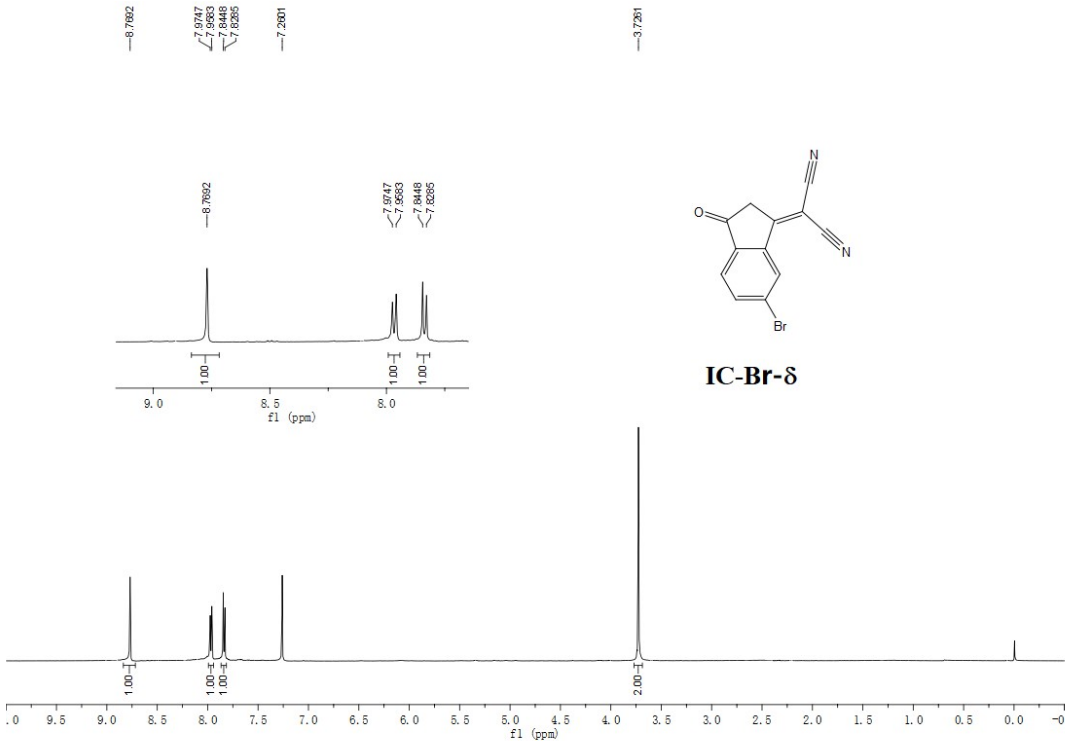

Fig.S5 The ^{1}H NMR spectrum of IC-Br-δ.

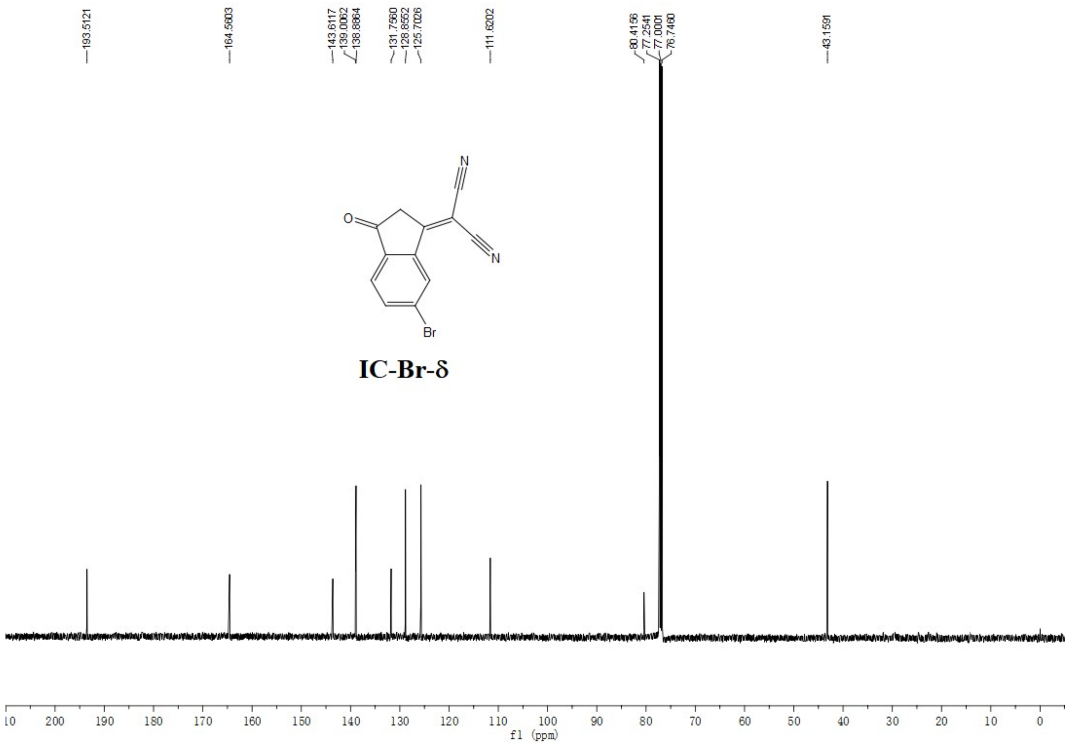

Fig.S6 The ^{13}C NMR spectrum of IC-Br-δ.

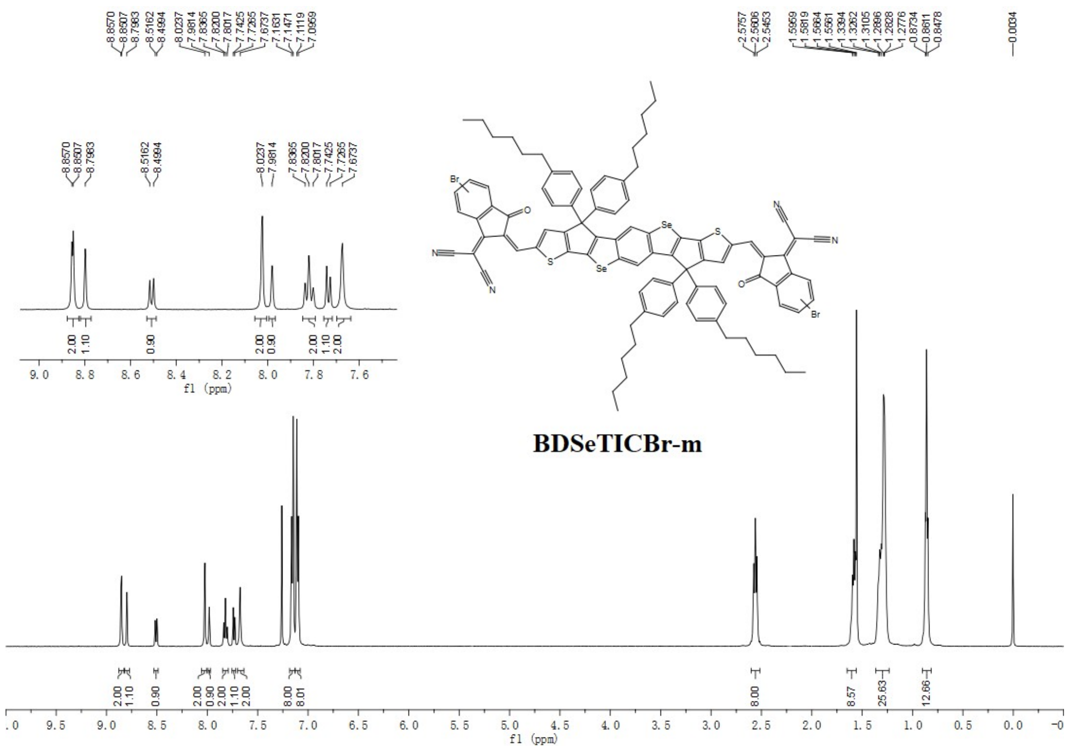

Fig.S7 The ^{1}H NMR spectrum of BDSeTICBr-m.

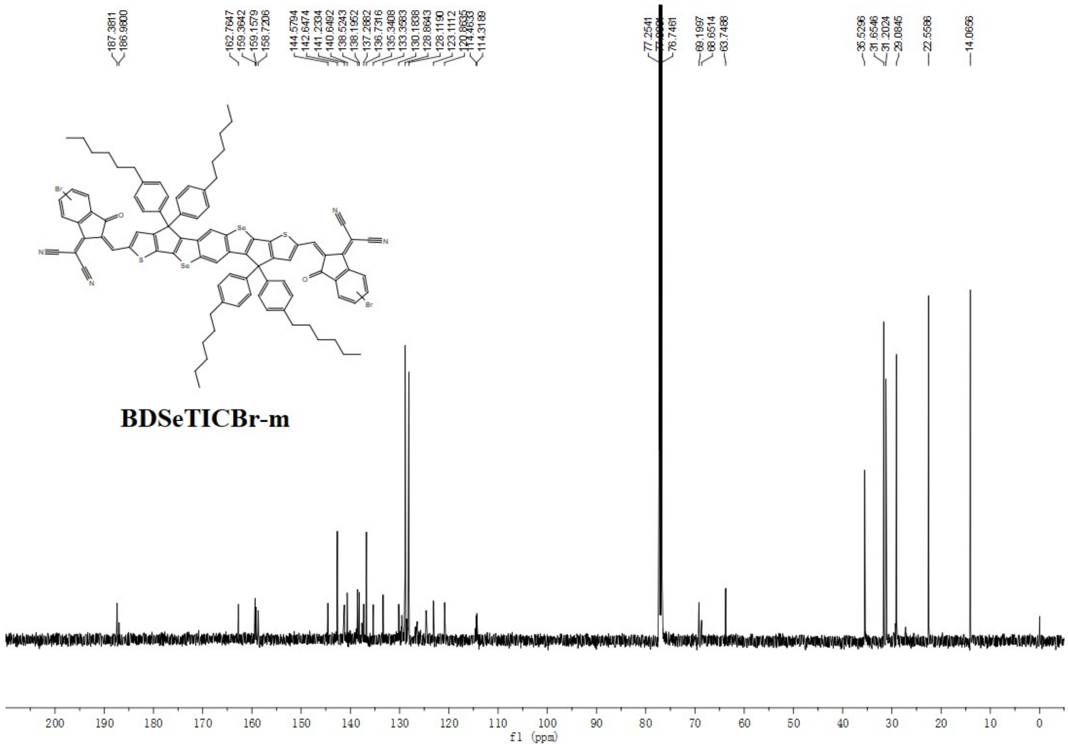

Fig.S8 The ^{13}C NMR spectrum of BDSeTICBr-m.

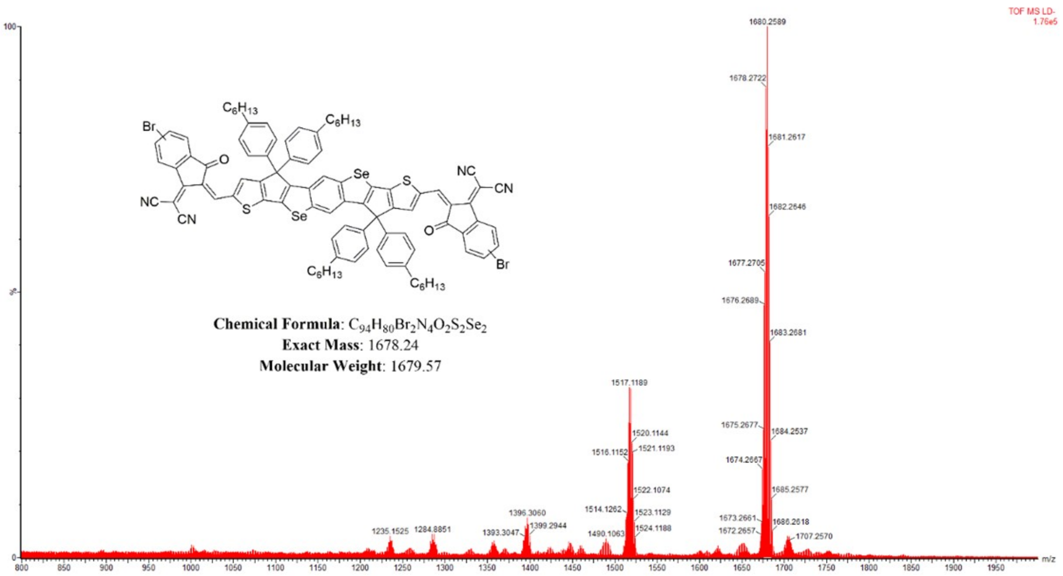

Fig.S9 The MALDI-TOF-MS result of BDSeTICBr-m.

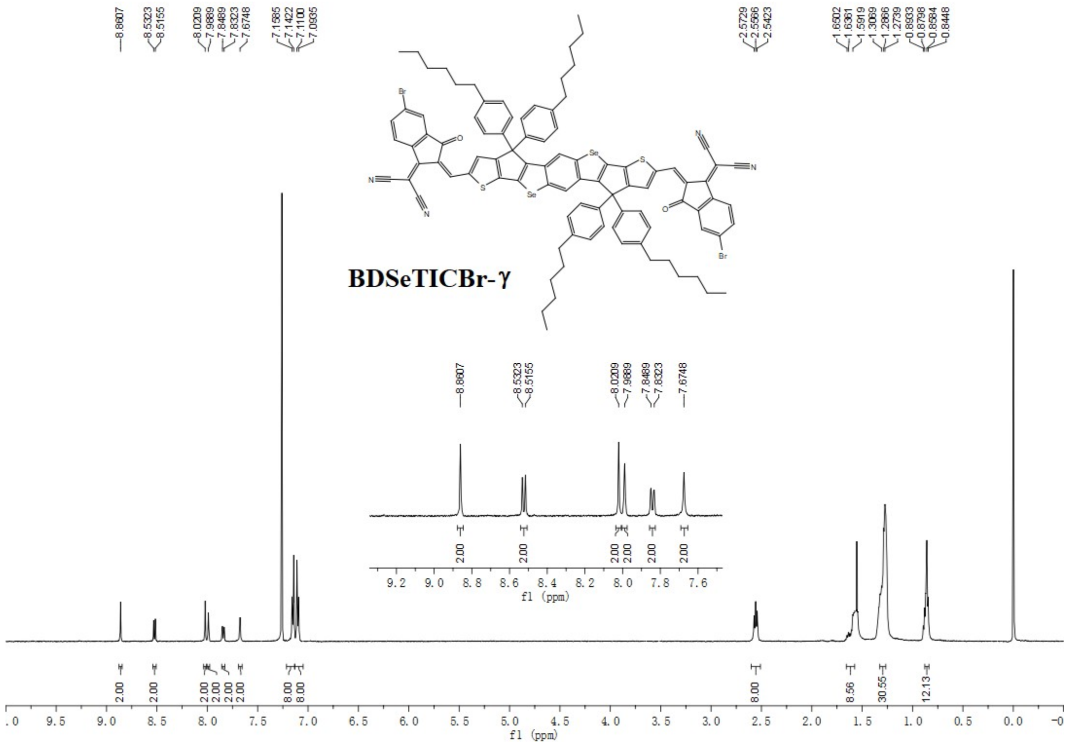

Fig.S10 The ^{1}H NMR spectrum of BDSeTICBr-γ.

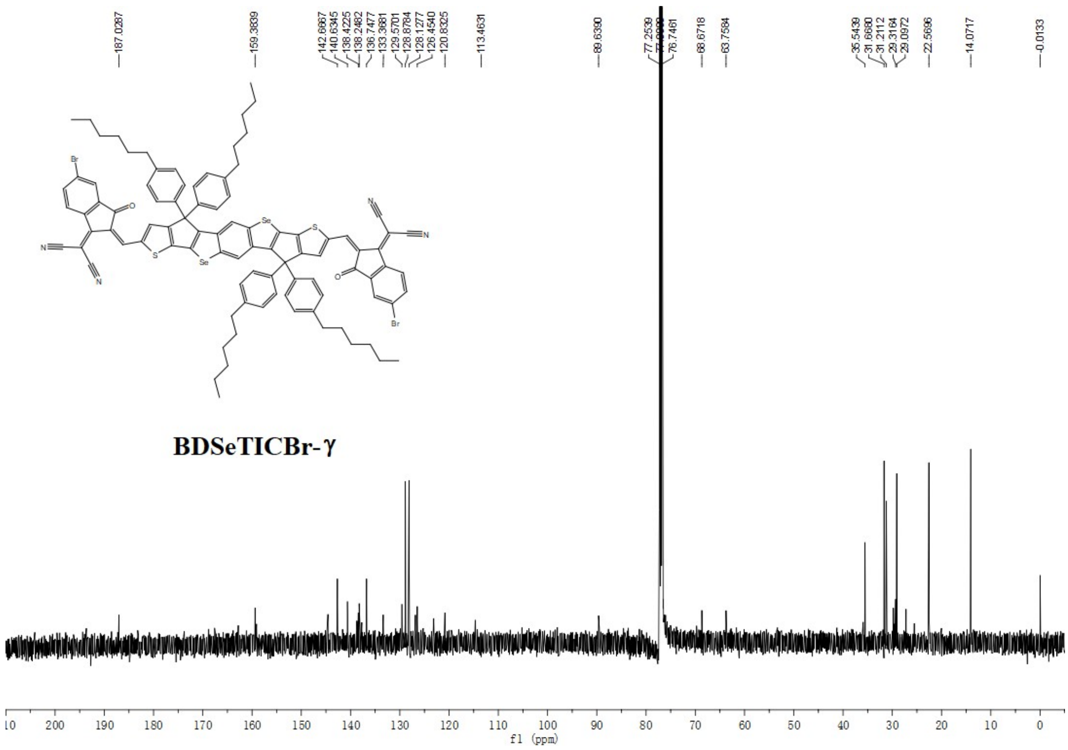

Fig.S11 The ^{13}C NMR spectrum of BDSeTICBr-γ.

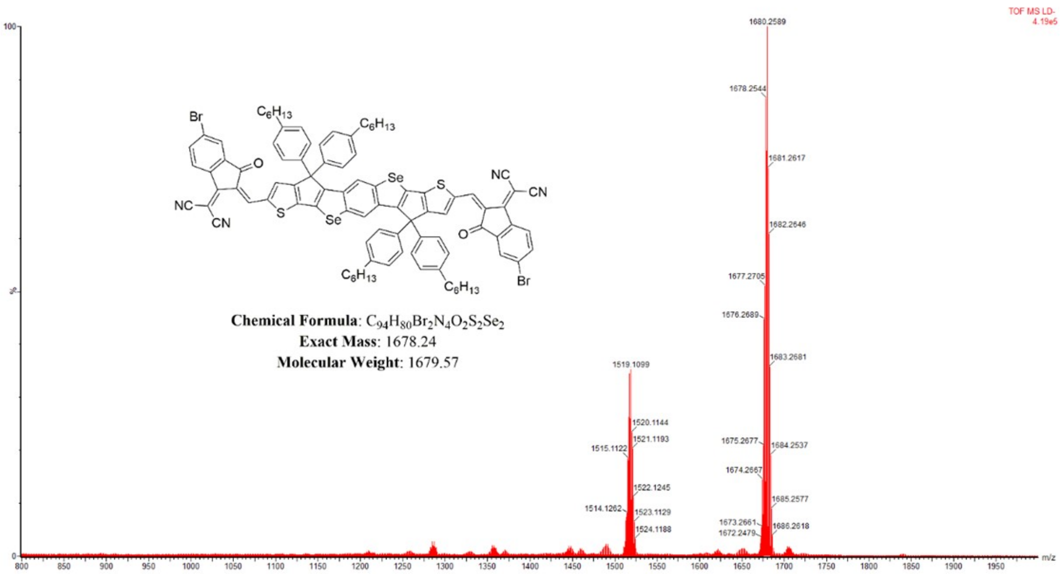

Fig.S12 The MALDI-TOF-MS result of BDSeTICBr-γ.

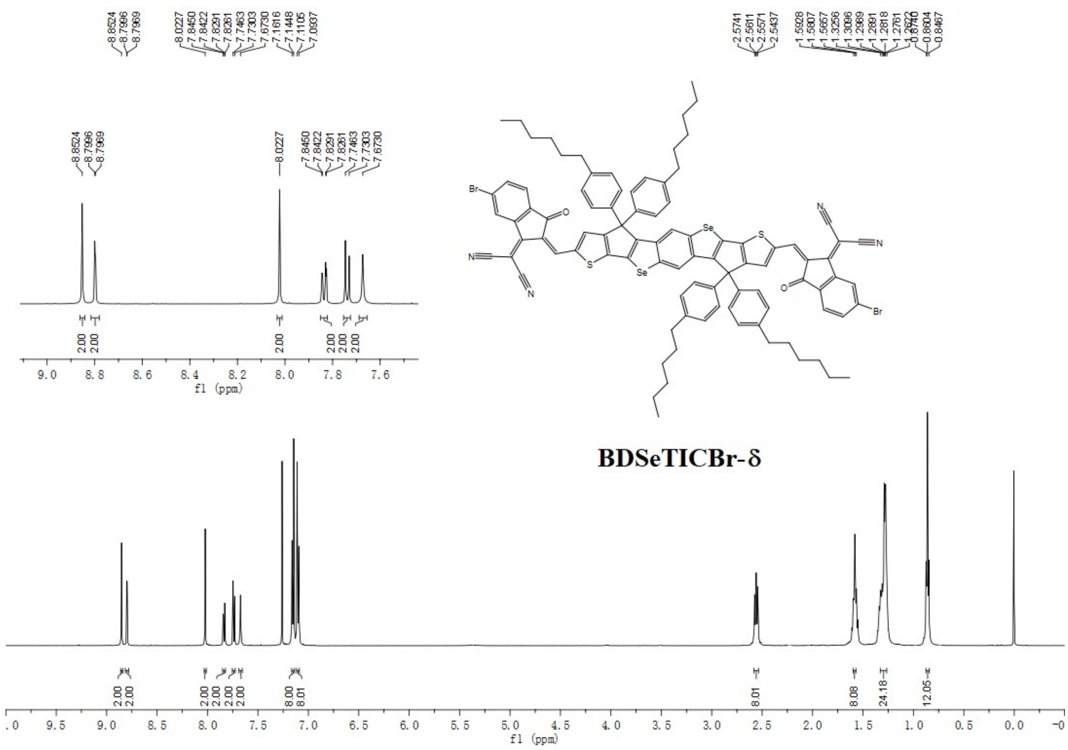

Fig.S13 The ^{1}H NMR spectrum of BDSeTICBr-δ.

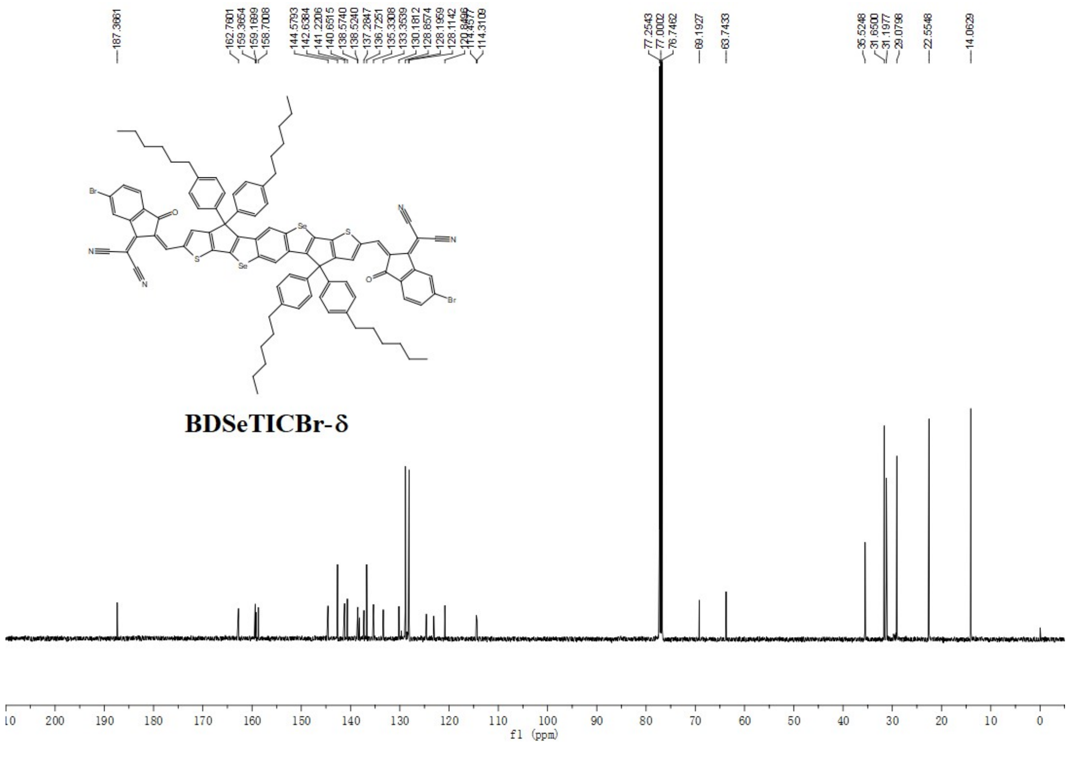

Fig.S14 The ^{13}C NMR spectrum of BDSeTICBr-δ.

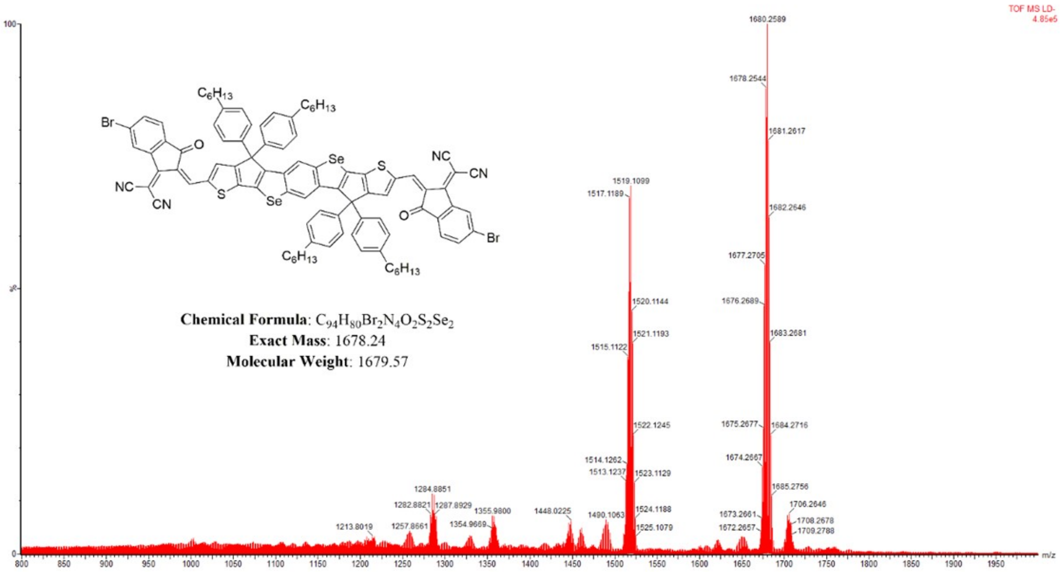

Fig.S15 The MALDI-TOF-MS result of BDSeTICBr-δ.

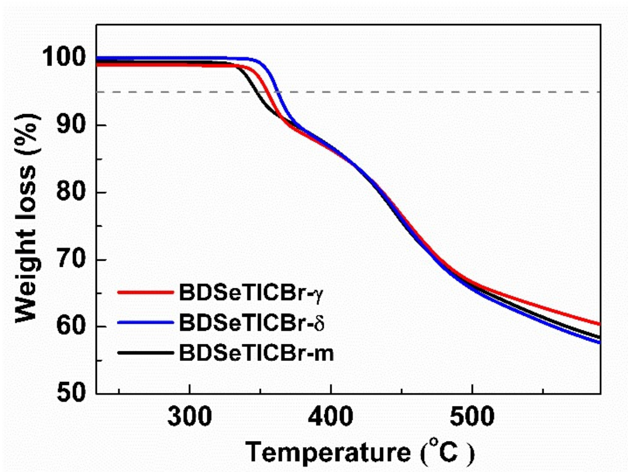

Fig.S16 Thermal gravimetric analysis (TGA) curves of BDSeTICBr-γ, BDSeTICBr-δ and BDSeTICBr-m at a heating rate of 10 $^{o}C\cdot min^{-1}$ under N_2.

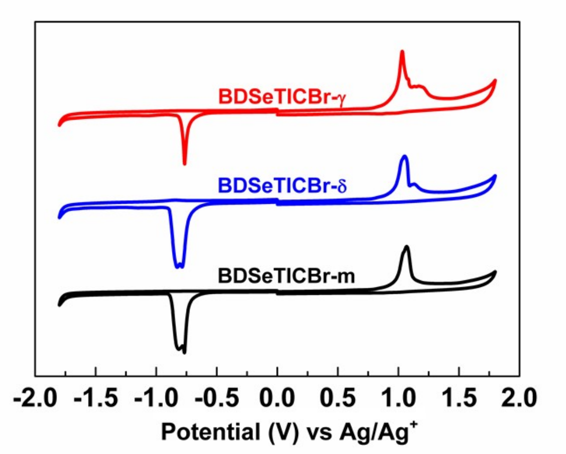

Fig.S17 Cyclic voltammogram of the BDSeTICBr-γ, BDSeTICBr-δ and BDSeTICBr-m film in 0.1 M Bu_4NPF_6 solution in CH_3CN with a scan rate of 80 $mV \cdot s^{-1}$.

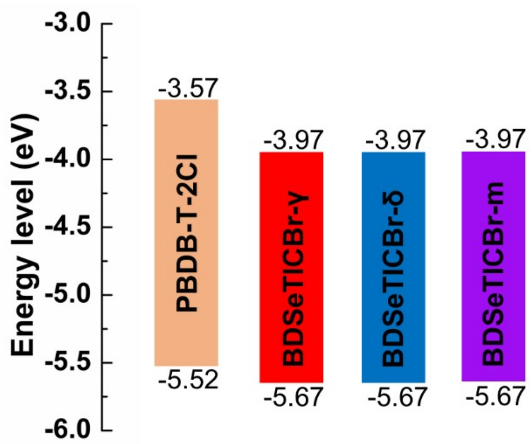

Fig.S18 The energy levels of the PBDB-T-2Cl, BDSeTICBr-γ, BDSeTICBr-δ and BDSeTICBr-m.

Table S1. The parameters on thermal stability, optical absorption and energy levels of BDSeTICBr-γ, BDSeTICBr-δ and BDSeTICBr-m.

Acceptor	T_d (°C)[a]	$\lambda_{s,\ max}$ (nm)[b]	$\lambda_{f,\ max}$ (nm)[c]	E_g^{opt} (nm)[d]	E_{HOMO} (eV)[e]	E_{LUMO} (eV)[e]	E_g^{cv} (eV)[f]
BDSeTICBr-γ	354.9	719	779	1.46	-5.67	-3.97	1.70
BDSeTICBr-δ	362.1	721	769	1.47	-5.67	-3.97	1.70
BDSeTICBr-m	347.4	721	765	1.48	-5.67	-3.97	1.70

[a] Decomposition temperature (5% weight loss) measured from TGA (in Fig. S17). [b] The maximum absorption in CB. [c] The maximum absorption in film. [d] Optical band gap calculated by E_g^{opt}=1240/$\lambda_{f,\ onset}$. [e] $E_{HOMO/LUMO}$ = e(- 4.7 - $E_{ox/red}$) (eV). [f] Bandgap estimated by E_g^{CV} = E_{LUMO} - E_{HOMO} (in Fig. S18).

Table S2. Photovoltaic parameters of the PBDB-T-2Cl:SMA devices with different D/A ratio (w/w) under AM 1.5G illumination.

Acceptor	D:A (w/w)	V_{oc} (V)	J_{sc} (mA cm^{-2})	*FF*	PCE (%)	Thickness (nm)
BDSeTICBr-γ	1:0.75	0.870 ± 0.002	11.40 ± 0.33	0.458 ± 0.004	4.54 ± 0.40	107 ± 2
	1:0.75	0.870 ± 0.002	12.51 ± 0.51	0.483 ± 0.005	5.26 ± 0.48	122 ± 2
	1:0.75	0.865 ± 0.003	10.11 ± 0.48	0.414 ± 0.003	3.62 ± 0.47	137 ± 2
	1:1	0.868 ± 0.003	12.31 ± 0.54	0.471 ± 0.006	5.03 ± 0.54	104 ± 2
	1:1[a]	0.866 ± 0.004	13.16 ± 0.63	0.482 ± 0.007	5.49 ± 0.67	119 ± 2
	1:1	0.862 ± 0.005	11.43 ± 0.49	0.435 ± 0.005	4.29 ± 0.67	134 ± 2
	1:1.25	0.851 ± 0.003	11.43 ± 0.56	0.442 ± 0.005	4.30 ± 0.51	98 ± 2
	1:1.25	0.846 ± 0.004	12.33 ± 0.41	0.477 ± 0.004	4.98 ± 0.55	113 ± 2
	1:1.25	0.840 ± 0.003	10.01 ± 0.36	0.432 ± 0.005	3.63 ± 0.37	128 ± 2
BDSeTICBr-δ	1:0.75	0.894 ± 0.002	12.41 ± 0.36	0.545 ± 0.006	6.05 ± 0.36	105 ± 2
	1:0.75	0.896 ± 0.003	13.78 ± 0.40	0.566 ± 0.007	6.98 ± 0.49	120 ± 2
	1:0.75	0.896 ± 0.003	14.01 ± 0.48	0.556 ± 0.007	6.98 ± 0.52	135 ± 2
	1:1	0.893 ± 0.003	14.33 ± 0.53	0.553 ± 0.005	7.08 ± 0.58	103 ± 2
	1:1[a]	0.895 ± 0.004	15.31 ± 0.37	0.575 ± 0.006	7.88 ± 0.33	118 ± 2
	1:1	0.896 ± 0.004	14.98 ± 0.45	0.560 ± 0.007	7.52 ± 0.42	133 ± 2
	1:1.25	0.886 ± 0.003	13.87 ± 0.34	0.522 ± 0.006	6.41 ± 0.40	100 ± 2
	1:1.25	0.888 ± 0.004	14.04 ± 0.55	0.547 ± 0.005	6.82 ± 0.50	115 ± 2
	1:1.25	0.890 ± 0.005	13.50 ± 0.43	0.509 ± 0.005	6.12 ± 0.44	130 ± 2
BDSeTICBr-m	1:0.75	0.906 ± 0.003	16.31 ± 0.35	0.547 ± 0.004	8.08 ± 0.38	109 ± 2

	1:0.75	0.908 ± 0.004	16.88 ± 0.37	0.563 ± 0.006	8.63 ±0.29	124 ± 2
	1:0.75	0.909 ± 0.004	16.51 ± 0.44	0.550 ± 0.005	8.25 ±0.41	139 ± 2
	1:1	0.905 ± 0.003	16.74 ± 0.50	0.564 ± 0.006	8.54 ± 0.54	108 ± 2
	1:1[a]	0.906 ± 0.002	17.32 ± 0.42	0.588 ± 0.005	9.23 ±0.48	123 ± 2
	1:1	0.907 ± 0.003	16.91 ± 0.61	0.562 ± 0.006	8.62 ± 0.54	138 ± 2
	1:1.25	0.901 ± 0.003	15.66 ± 0.53	0.540 ± 0.004	7.62 ± 0.57	106 ± 2
	1:1.25	0.901 ± 0.003	16.51 ± 0.48	0.551 ± 0.005	8.20 ± 0.41	121 ± 2
	1:1.25	0.892 ± 0.004	15.99 ± 0.59	0.533 ± 0.006	7.60 ± 0.54	136 ± 2

[a] The spinning speed was 600 rpm and the spinning time was 60 s.

Table S3. Photovoltaic parameters of the PBDB-T-2Cl:SMA (1:1, w/w) devices with the additive of 1-chloronaphthalene (CN) at different volumes in CB under AM 1.5G illumination.

Acceptor	**CN (%, v/v)**	**V_{oc} (V)**	**J_{sc} (mA cm^{-2})**	**FF**	**PCE (%)**
BDSeTICBr-γ	w/o	0.866 ± 0.004	13.16 ± 0.63	0.482 ± 0.007	5.49 ± 0.67
	0.1	0.889 ± 0.004	13.56 ± 0.37	0.491 ± 0.005	5.92 ± 0.41
	0.25	0.890 ± 0.003	14.25 ± 0.67	0.498 ± 0.008	6.29 ± 0.54
	0.5	0.893 ± 0.002	15.92 ± 0.69	0.530 ± 0.004	7.53 ± 0.38
	0.75	0.894 ± 0.002	15.03 ± 0.69	0.547 ± 0.004	7.35 ± 0.23
	1	0.895 ± 0.002	14.17 ± 0.69	0.560 ± 0.003	7.10 ± 0.23
BDSeTICBr-δ	w/o	0.895 ± 0.004	15.31 ± 0.37	0.575 ± 0.006	7.88 ± 0.33
	0.1	0.896 ± 0.003	15.21 ± 0.21	0.554 ± 0.002	7.55 ± 0.29
	0.25	0.896 ± 0.003	15.67 ± 0.31	0.581 ± 0.006	8.16 ± 0.45
	0.5	0.898 ± 0.001	17.83 ± 0.72	0.618 ± 0.005	9.88 ± 0.61
	0.75	0.900 ± 0.001	17.26 ± 0.44	0.611 ± 0.005	9.49 ± 0.59
	1	0.902 ± 0.002	16.67 ± 0.53	0.603 ± 0.003	9.07 ± 0.39
BDSeTICBr-m	w/o	0.906 ± 0.002	17.32 ± 0.42	0.588 ± 0.005	9.23 ±0.48
	0.1	0.906 ± 0.002	17.33 ± 0.29	0.571 ± 0.004	8.97 ± 0.39
	0.25	0.907 ± 0.003	17.15 ± 0.11	0.566 ± 0.003	8.80 ± 0.26
	0.5	0.905 ± 0.003	16.79 ± 0.57	0.570 ± 0.002	8.66 ± 0.38
	0.75	0.906 ± 0.002	16.33 ± 0.44	0.568 ± 0.003	8.40 ± 0.49
	1	0.905 ± 0.003	16.02 ± 0.57	0.572 ± 0.003	8.29 ± 0.38

Table S4. Photovoltaic parameters of the PBDB-T-2Cl:SMA (1:1, w/w) devices (under AM 1.5G illumination) with films thermally annealed at different temperatures.

Acceptor	**Temperature (^{o}C)**	**V_{oc} (V)**	**J_{sc} (mA cm^{-2})**	**FF**	**PCE (%)**
BDSeTICBr-γ	w/o	0.866 ± 0.004	13.16 ± 0.63	0.482 ± 0.007	5.49 ± 0.67
	100	0.880 ± 0.003	13.51 ± 0.51	0.512 ± 0.003	6.08 ± 0.50
	120	0.878 ± 0.002	13.22 ± 0.36	0.523 ± 0.004	6.07 ± 0.41
	140	0.876 ± 0.002	13.44 ± 0.49	0.531 ± 0.004	6.25 ± 0.44
	160	0.876 ± 0.003	13.25 ± 0.60	0.522 ± 0.005	6.06 ± 0.52
	180	0.874 ± 0.003	13.11 ± 0.55	0.520 ± 0.006	5.96 ± 0.48
BDSeTICBr-δ	w/o	0.895 ± 0.004	15.31 ± 0.37	0.575 ± 0.006	7.88 ± 0.33
	100	0.893 ± 0.003	17.26 ± 0.36	0.595 ± 0.005	9.17 ± 0.41
	120	0.892 ± 0.002	18.01 ± 0.62	0.605 ± 0.004	9.72 ± 0.68
	140	0.890 ± 0.003	18.31 ± 0.63	0.620 ± 0.007	10.10 ± 0.41
	160	0.886 ± 0.002	18.36 ± 0.52	0.633 ± 0.004	10.29 ± 0.47
	180	0.880 ± 0.002	18.01 ± 0.31	0.592 ± 0.004	9.38 ± 0.39
BDSeTICBr-m	0	0.906 ± 0.002	17.32 ± 0.42	0.588 ± 0.005	9.23 ±0.48
	100	0.901 ± 0.004	18.82 ± 0.63	0.608 ± 0.003	10.31 ± 0.58
	120	0.899 ± 0.002	19.02 ± 0.55	0.617 ± 0.002	10.54 ± 0.42
	140	0.896 ± 0.002	19.52 ± 0.39	0.622 ± 0.005	10.87 ± 0.33
	160	0.893 ± 0.003	19.33 ± 0.17	0.657 ± 0.006	11.34 ± 0.28
	180	0.881 ± 0.004	18.60 ± 0.67	0.591 ± 0.007	9.68 ± 0.31

Table S5. Photovoltaic parameters of the PBDB-T-2Cl:BDSeTICBr-γ (1:1, w/w) devices (under AM 1.5G illumination) processed from the CB solution with 0.5% CN (v/v) and later thermally annealed at different temperatures.

Acceptor	**Temperature (^{o}C)**	**V_{oc} (V)**	**J_{sc} (mA cm^{-2})**	**FF**	**PCE (%)**
BDSeTICBr-γ	w/o	0.893 ± 0.002	15.92 ± 0.69	0.530 ± 0.004	7.53 ± 0.38
	100	0.880 ± 0.003	16.29 ± 0.40	0.565 ± 0.005	8.10 ± 0.49
	120	0.889 ± 0.002	16.59 ± 0.21	0.561 ± 0.006	8.27 ± 0.31
	140	0.892 ± 0.002	16.37 ± 0.56	0.571 ± 0.003	8.34 ± 0.41
	160	0.886 ± 0.002	17.70 ± 0.28	0.588 ± 0.003	9.22 ± 0.55
	180	0.865 ± 0.003	16.59 ± 0.54	0.533 ± 0.005	7.65 ± 0.63

Table S6. Photovoltaic parameters of the PBDB-T-2Cl: BDSeTICBr-δ (1:1, w/w) devices (under AM 1.5G illumination) processed from the CB solution with 0.5% CN (v/v) and later thermally annealed at different temperatures.

Acceptor	**Temperature (^{o}C)**	**V_{oc} (V)**	**J_{sc} (mA cm^{-2})**	**FF**	**PCE (%)**
BDSeTICBr-δ	w/o	0.898 ± 0.001	17.83 ± 0.72	0.618 ± 0.005	9.88 ± 0.61
	100	0.886 ± 0.002	17.33 ± 0.49	0.599 ± 0.004	9.20 ± 0.40
	120	0.882 ± 0.003	17.85 ± 0.41	0.602 ± 0.006	9.47 ± 0.38
	140	0.880 ± 0.003	18.11 ± 0.55	0.603 ± 0.005	9.61 ± 0.57
	160	0.878 ± 0.004	18.68 ± 0.65	0.600 ± 0.004	9.84 ± 0.43
	180	0.874 ± 0.002	18.31 ± 0.60	0.577 ± 0.003	9.23 ± 0.54

Table S7. Photovoltaic parameters of the PBDB-T-2Cl: BDSeTICBr-m (1:1, w/w) devices (under AM 1.5G illumination) processed from the CB solution with 0.5% CN (v/v) and later thermally annealed at different temperatures.

Acceptor	Temperature (°C)	V_{oc} (V)	J_{sc} (mA cm^{-2})	FF	PCE (%)
BDSeTICBr-m	w/o	0.906 ± 0.002	17.33 ± 0.29	0.571 ± 0.004	8.97 ± 0.39
	100	0.891 ± 0.002	16.97 ± 0.31	0.566 ± 0.003	8.56 ± 0.38
	120	0.886 ± 0.003	17.11 ± 0.45	0.571 ± 0.005	8.66 ± 0.43
	140	0.881 ± 0.002	17.46 ± 0.58	0.580 ± 0.006	8.92 ± 0.52
	160	0.878 ± 0.003	17.82 ± 0.57	0.599 ± 0.004	9.37 ± 0.50
	180	0.870 ± 0.004	17.31 ± 0.42	0.591 ± 0.004	8.90 ± 0.47

Table S8. The optimized photovoltaic parameters of the PBDB-T-2Cl: SMA (1:1, w/w) devices processing with the additive CN (v/v, in CB), TA and CN+TA under AM 1.5G illumination.

Acceptor	Processings	V_{oc} (V)	J_{sc} (mA cm^{-2})	FF	PCE (%)	Thickness (nm)
BDSeTICBr-γ	w/o	0.866 ± 0.004	13.16 ± 0.63	0.482 ± 0.007	5.49 ± 0.67	119 ± 2
	160 °C	0.862 ± 0.003	13.55 ± 0.66	0.500 ± 0.006	5.84 ± 0.63	119 ± 2
	0.5% CN	0.893 ± 0.002	15.92 ± 0.69	0.530 ± 0.004	7.53 ± 0.38	116 ± 2
	0.5% CN + 160 °C	0.886 ± 0.002	17.70 ± 0.28	0.588 ± 0.003	9.22 ± 0.55	115 ± 2
BDSeTICBr-δ	w/o	0.895 ± 0.004	15.31 ± 0.37	0.575 ± 0.006	7.88 ± 0.33	118 ± 2
	160 °C	0.886 ± 0.002	18.36 ± 0.52	0.633 ± 0.004	10.29 ± 0.47	118 ± 2
	0.5% CN	0.898 ± 0.001	17.83 ± 0.72	0.618 ± 0.005	9.88 ± 0.61	115 ± 2
	0.5% CN + 160 °C	0.878 ± 0.004	18.68 ± 0.65	0.600 ± 0.004	9.84 ± 0.43	114 ± 2
BDSeTICBr-m	w/o	0.910 ± 0.003	16.29 ± 0.33	0.549 ±0.004	8.14 ± 0.37	123 ± 2
	160 °C	0.893 ± 0.003	19.33 ± 0.17	0.657 ± 0.006	11.34 ± 0.28	122 ± 2
	0.1% CN	0.906 ± 0.002	17.33 ± 0.29	0.571 ± 0.004	8.97 ± 0.39	120 ± 2
	0.1% CN + 160 °C	0.878 ± 0.003	17.82 ± 0.57	0.599 ± 0.004	9.37 ± 0.50	120 ± 2

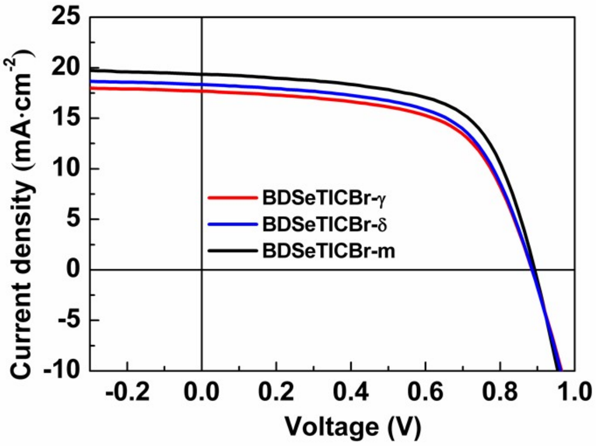

Fig.S19 The typical *J-V* curves of the optimized PBDB-T-2Cl: SMA PSCs under AM 1.5G irradiation.

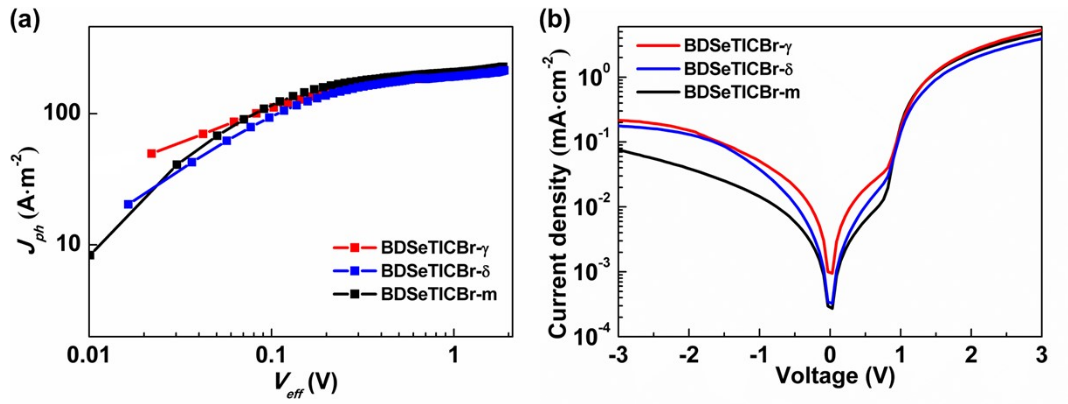

Fig.S20 Photogenerated current density versus effective voltage curves under AM 1.5G illumination (a) and *J-V* curves from -3 V to +3 V in dark (b).

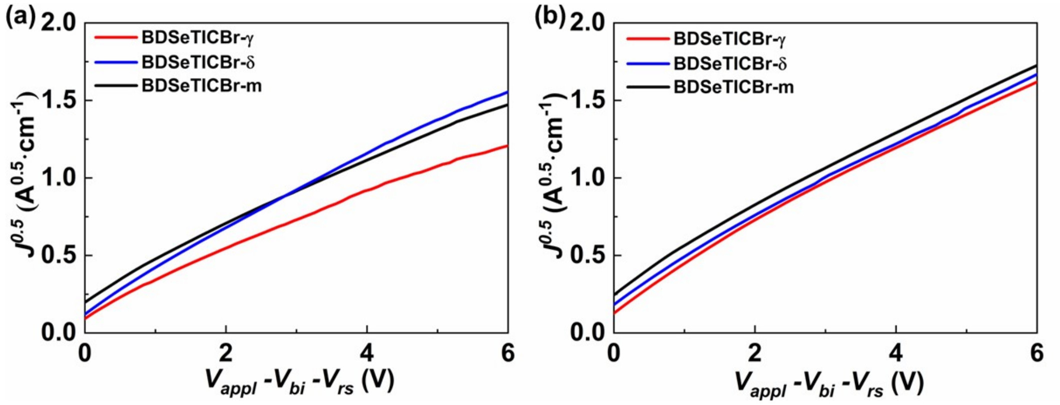

Fig.S21 $J^{0.5}$ vs V ($V = V_{appl} - V_{bi} - V_{rs}$) plots for electron-only (a) and hole-only (b) devices of the PBDB-T-2Cl:SMA blends.

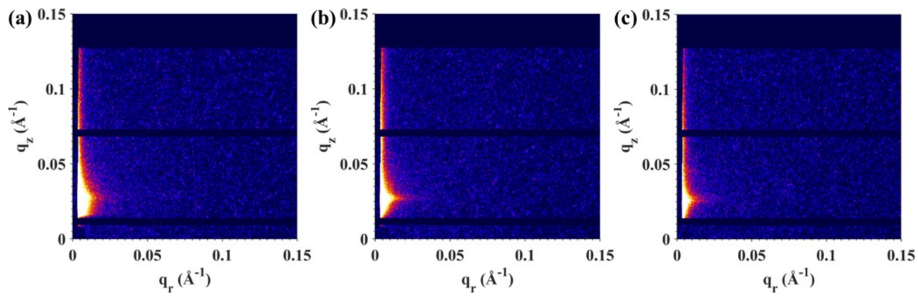

Fig.S22 GISAXS patterns of the PBDB-T-2Cl:BDSeTICBr-γ (a), PBDB-T-2Cl:BDSeTICBr-δ (b) and PBDB-T-2Cl:BDSeTICBr-m (c) film.

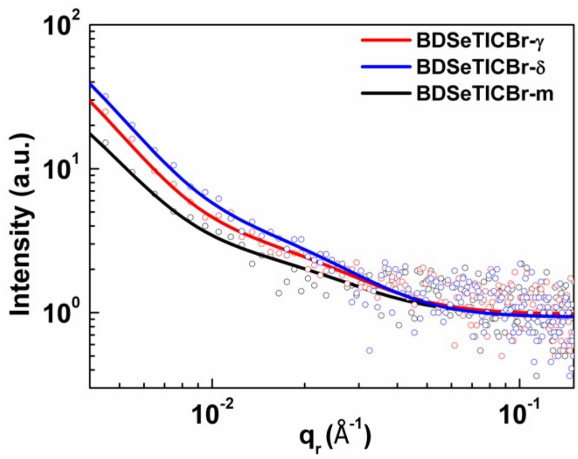

Fig.S23 GISAXS in-plane profiles of the PBDB-T-2Cl:SMA blend films and their model fittings with the Debye-Anderson-Brumberger (DAB) model.

Table S9. The calculated domain sizes from GISAXS within the PBDB-T-2Cl:BDSeTICBr-γ, PBDB-T-2Cl:BDSeTICBr-δ and PBDB-T-2Cl:BDSeTICBr-m films.[a]

Film	Intermixing phase (nm)	Acceptor Domain size (nm)
BDSeTICBr-γ blend	31.9	15.0
BDSeTICBr-δ blend	30.5	16.0
BDSeTICBr-m blend	29.6	14.9

[a] The domain sizes were calculated according to the GISAXS profiles fitted with the Debye-Anderson-Brumberger (DAB) model.

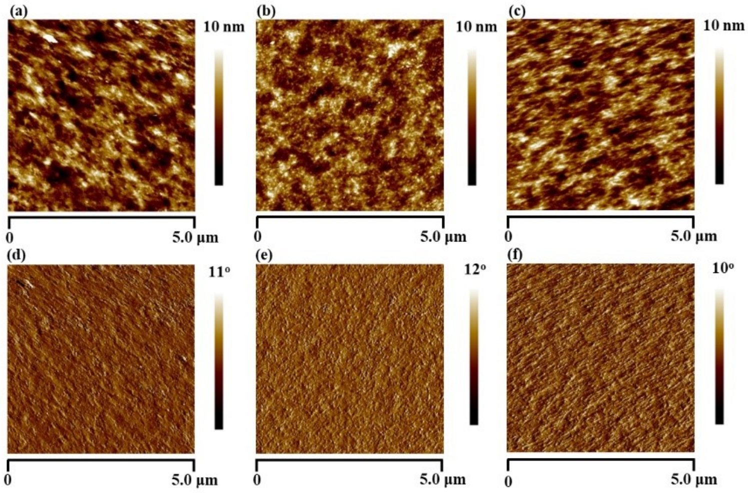

Fig.S24 AFM height images (a), (b), (c) and phase images (d), (e), (f) for, the PBDB-T-2Cl: BDSeTICBr-γ film, PBDB-T-2Cl: BDSeTICBr-δ film and PBDB-T-2Cl: BDSeTICBr-m film, respectively.

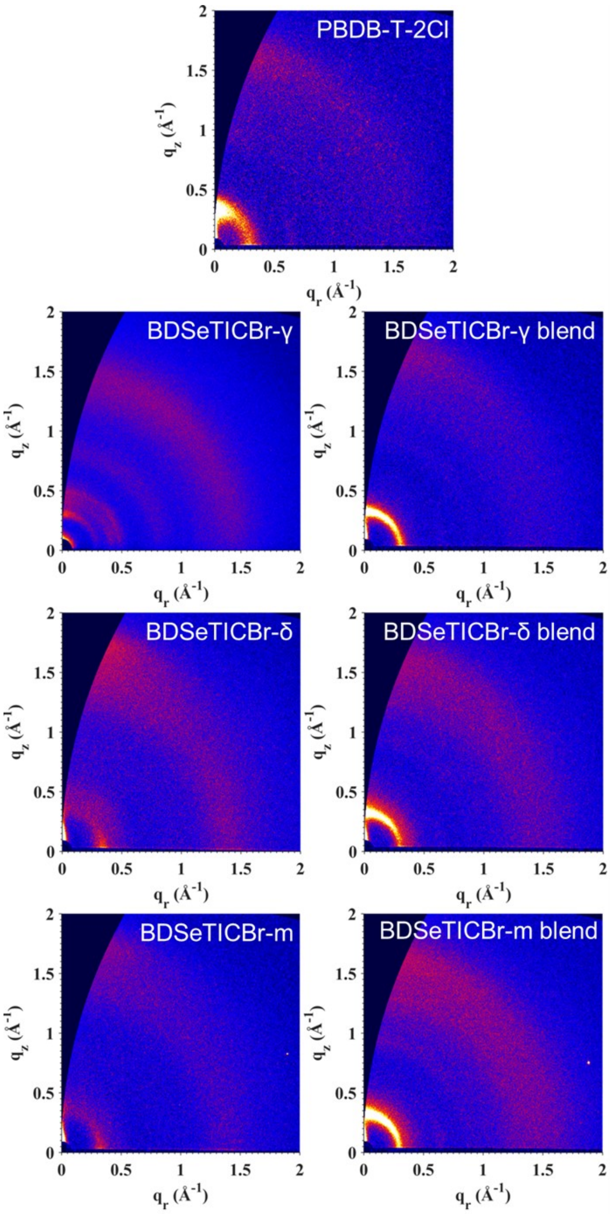

Fig.S25 GIWAXS scattering patterns of the neat films of the PBDB-T-2Cl, BDSeTICBr-γ, BDSeTICBr-δ and BDSeTICBr-m and their PBDB-T-2Cl:SMA blend films.

Table S10. GIWAXS characteristics of the neat films of the PBDB-T-2Cl, BDSeTICBr-γ, BDSeTICBr-δ and BDSeTICBr-m and their PBDB-T-2Cl:SMA blend films.

Direction	Film	(100)		(200)		(010)	
		q (Å^{-1})	d (Å)	q (Å^{-1})	d (Å)	q (Å^{-1})	d (Å)
In plane (IP)	PBDB-T-2Cl	0.285	22.0	0.650	9.67	-[a]	-[a]
	BDSeTICBr-γ	0.280	22.4			1.45	4.33
	BDSeTICBr-δ	0.338	18.6			1.39	4.52
	BDSeTICBr-m	0.320	19.6			1.46	4.30
	BDSeTICBr-γ blend	0.296	21.2	0.648	9.70	1.45	4.33
	BDSeTICBr-δ blend	0.296	21.2	0.615	10.2	1.39	4.52
	BDSeTICBr-m blend	0.295	21.3	0.648	9.70	1.49	4.21
Out of plane (OOP)	PBDB-T-2Cl	0.328	19.1			1.67	3.76
	BDSeTICBr-γ	0.308	20.4			1.45	4.33
	BDSeTICBr-δ	0.366	17.2			1.73	3.63
	BDSeTICBr-m	0.366	17.2			1.79	3.51
	BDSeTICBr-γ blend	0.328	19.1			1.67	3.76
	BDSeTICBr-δ blend	0.328	19.1			1.67	3.76
	BDSeTICBr-m blend	0.328	19.1			1.67	3.76

[a] Not available.

6. References.

(1) Yang, F.; Li, C.; Lai, W.; Zhang, A.; Huang, H.; Li, W., *Mater. Chem. Front.* **2017**, *1*, 1389-1395.

(2) Wan, S. S.; Chang, C.; Wang, J. L.; Yuan, G. Z.; Wu, Q.; Zhang, M.; Li, Y., *Solar RRL* **2018**, *8*, 1702870.

(3) Fan, Q.; Zhu, Q.; Xu, Z.; Su, W.; Chen, J.; Wu, J.; Guo, X.; Ma, W.; Zhang, M.; Li, Y., *Nano Energy* **2017**,*139*, 1336-1343.

(4) Sun, Y.; Seo, J. H.; Takacs, C. J.; Seifter, J.; Heeger, A. J., *Adv. Mater.* **2011**, *23*, 1679-83.